Diamond & Related Materials 120 (2021) 108587

Contents lists available at ScienceDirect

Diamond & Related Materials

journal homepage: www.elsevier.com/locate/diamond

Enhancement of concentration of XeV and GeV centers in microcrystalline diamond films through He^+ irradiation

T. Chakraborty [a,b,*], K.J. Sankaran [a,b,1], K. Srinivasu [c], R. Nongjai [d], K. Asokan [d], C.H. Chen [c], H. Niu [c], K. Haenen [a,b]

[a] Institute for Materials Research (IMO), Hasselt University, 3590 Diepenbeek, Belgium
[b] IMOMEC, IMEC vzw, 3590 Diepenbeek, Belgium
[c] Accelerator Laboratory, Nuclear Science and Technology Development Center, National Tsing Hua University, Hsinchu 30013, Taiwan
[d] Materials Science Group, Inter-University Accelerator Centre, New Delhi 110 067, India

ARTICLE INFO

Keywords:
Synthetic diamond
Nanodiamonds
Chemical vapor deposition
Optical spectroscopy
Ion implantation
Raman spectroscopy

ABSTRACT

Atomic defect centers in diamond have been widely exploited in numerous quantum applications like quantum information, sensing, quantum photonics and so on. In this context, there is always a requirement to improve and optimize the preparation procedure to generate the defect centers in controlled fashion, and to explore new defect centers which can have the potential to overcome the current technological challenges. Through this work we report enhancing the concentration of Ge and Xe vacancy centers in microcrystalline diamond (MCD) by means of He^+ irradiation. We have demonstrated controlled growth of MCD by chemical vapor deposition (CVD) and implantation of Ge and Xe ions into the CVD-grown samples. MCDs were irradiated with He^+ ions and characterized through optical spectroscopy measurements. Recorded photoluminescence results revealed a clear signature of enhancement of the Xe-related and Ge vacancies in MCDs.

1. Introduction

In the last few decades, there have been notable advancements in the direction of synthesizing and growing diamond crystals in a controlled way which on one hand has boosted up the progress in material science and solid state physics [1,2], and on the other hand, has privileged the quantum revolution which exploits the atomic defect centers in diamond [3,4]. The Nitrogen vacancy (NV) center in diamond is established as a promising atomic defect center in diamond which has exhibited promising applications in quantum information processing [5,6], magnetometry [7,8], bio-sensing [9,10], thermometry [11,12] and so on. However, the NV center has certain disadvantages: the photoluminescence (PL) signal from the zero phonon line (ZPL) has only a contribution of ~4% to the total spectrum where the rest of the signal is in phononic sidebands. Moreover, the NV center possesses a permanent dipole moment which makes it sensitive to external electrostatic fields. This is responsible for the spectral diffusion of the NV optical transitions and hence that affects the efficiency of generating single photons [13,14].

Elements of group IV of the periodic table, namely the SiV [15–17] and GeV [18–20] centers in diamond have the potential to overcome the above-mentioned issues. The structure of these vacancy centers is inversion symmetric which makes them less susceptible to electrostatic fields. This results in a bright and narrowband emission into the ZPL and indistinguishability of the single photons emitted from multiple centers [19]. Specifically, the GeV center has certain advantages over the SiV center: because there is considerable probability that the excited state of the SiV center decays through certain nonradiative pathways, the SiV center has lesser quantum efficiency than that of the GeV center [21]. These excellent spectral and spin properties make the GeV center a suitable system for quantum photonic and plasmonic applications [22,23]. In this context, a constant experimental progress on the preparation procedure and optimization of the growth process are necessary to prepare GeV centers in diamond in a deterministic way, which is one of the main focuses of the present study.

In certain optical applications, it is advantageous to find out single photon sources which emit in the far-infrared regions. For instance, in fiber optic based communication the attenuation through silica glass

* Corresponding author at: QuTech and Kavli Institute of Nanoscience, Delft University of Technology, 2600 GA Delft, the Netherlands.
E-mail address: t.chakraborty-1@tudelft.nl (T. Chakraborty).
[1] Present address: CSIR-Institute of Minerals and Materials Technology, Bhubaneswar 751013, India.

https://doi.org/10.1016/j.diamond.2021.108587
Received 3 May 2021; Received in revised form 1 August 2021; Accepted 25 August 2021
Available online 8 September 2021

fibers is considerably less in the infrared and far-infrared region in comparison to that in the visible range [24]. The Xe-related vacancy (XeV) center in diamond, which exhibits ZPLs at ~811 nm and ~795 nm, fulfil the above criterion. The XeV center is less investigated defect center in diamond [25–27], whose exact crystallographic structure and spin properties are still to be explored. Considering its possible application in optical technology, we have focused on preparation and spectroscopic study of the XeV center.

A widely used technique to create NV centers in diamond is through implanting high energy (~MeV) nitrogen ions into the diamond substrate [28,29] and subsequent annealing around 800 °C [30] in ultra high vacuum (air pressure $\sim 10^{-10}$ mbar). However, such implantation technique requires a highly sophisticated ion accelerator, ion-focusing technique and supporting experimental set-up [29,30] that is not easy to assemble, which hinders the easy production of NV centers. An alternative efficient procedure to make large scale production of vacancies is by performing low energy ion implantation and subsequently irradiating the diamond substrate by low energy ions like protons and He^+ ions, which requires substantially less incident beam energy (<1 keV) [31]. He being a chemically inert gas, neutralization of the ions and embedment of He atoms in diamond hardly affects the photo-physical properties of the NV center [32]. He^+ ions are proven to be more efficient than protons in terms of creating larger number of vacancies [31]. With He^+ irradiation, the larger number of vacancies can be created with an implantation energy two orders of magnitude less than what is required for electron [33–35] and H^+ implantation. He^+ beams with sufficient power required for creating vacancies can be generated using an RF ion source which can produce a current of two order magnitude higher than what can be generated for H^+ ions from an accelerator [35].

Earlier reports have demonstrated large scale preparation of stable NV centers in synthetic microcrystalline diamond (MCD) [32] with He^+ irradiation and the efficiency of the process has been investigated as a function of ion beam energy and dose [36]. We have investigated the effectiveness of He^+ irradiation on enhancing the concentration of the GeV and XeV centers through this work. We demonstrate controlled growth of MCD, creation of GeV and XeV centers through ion implantation, spectroscopic investigation of the created centers and the study of the effect of He^+ irradiation on the optical properties of the centers. We create the GeV and XeV centers in MCDs as the preparation of color centers in MCD thin films is much cheaper compared to the single-crystalline diamond (SCD) layers. MCD films are grown on cheap materials like Si substrates whereas to grow an SCD layer, one needs SCD substrates which are much expensive. As a host of the color centers, MCDs are excellent candidate for applications in bio-imaging, targeted drug delivery, sensing of temperature, spatial orientation, strain, pressure, magnetic and electric fields [9,32,37].

2. Materials and methods

2.1. Growth of diamond films

MCD films of about 250 nm thickness were deposited onto Si (100) substrates using linear antenna microwave plasma enhanced chemical vapor deposition. A gas mixture of CH_4 and H_2 with flow rates of 30 and 270 sccm (CH_4/H_2 = 10/90), respectively, was excited by 2800 W microwave power and at a total pressure of 0.18 Torr to grow the MCD

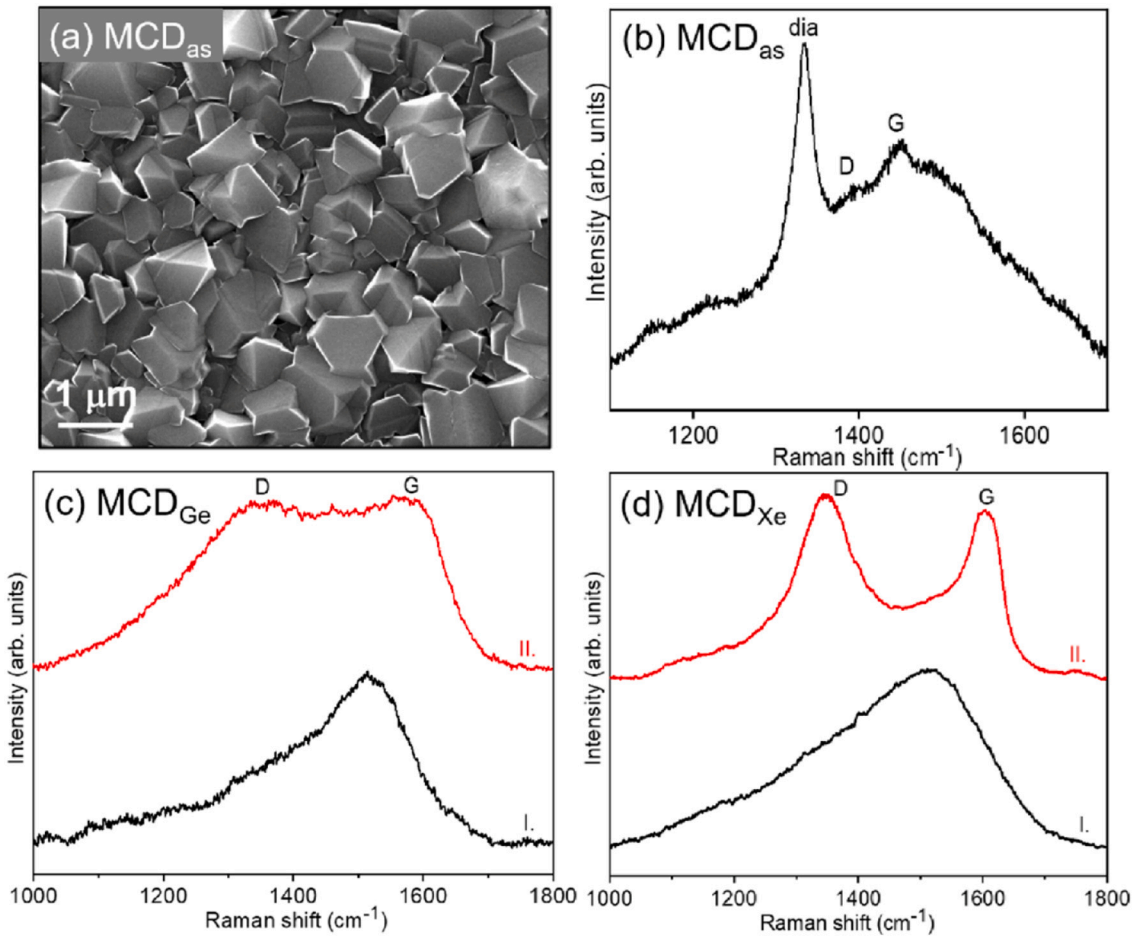

Fig. 1. (a) SEM micrograph and (b) Raman spectrum of as-deposited MCD films. Raman spectra of (I) as-implanted and (II) He-ion irradiated and annealed (c) Ge and (d) Xe-ion implanted MCD films.

films. The film thickness was monitored by in-situ laser reflection interferometry. The substrates were heated up due to the bombardment of the plasma species. The substrate temperature was about 350 °C, which was measured by a single color optical pyrometer [38]. The pre-seeding process on the Si substrates was performed by spin coating a water-based state-of-the-art colloidal suspension of ultra-dispersed 6-7 nm sized detonation diamond particles. The scanning electron microscopy (FEI Quanta 200 FEG scanning electron microscope operated at 15 kV) image shown in Fig. 1(a) illustrates that the as-deposited MCD films have uniform coverage of 1 μm sized faceted diamond grains. Fig. 1 (b) shows the Raman spectrum (a Horiba Jobin Yvon T64000 Raman spectrometer equipped with a BXFM Olympus 9/128 microscope in combination with a Horiba JY Symphony CCD detector with a 488 nm Lexell SHG laser) of as-deposited MCD films, revealing a sharp peak at 1332 cm^{-1}, representing sp^3-diamond, the broad bands at ~1390 cm^{-1} and ~1450 cm^{-1} representing the disordered carbon (D) and graphitic (G) phases, respectively.

2.2. Xe and Ge ion implantation and He^+ irradiation

Xe and Ge ion implantations into MCD films were carried out using the low energy ion beam facilities available at Inter University Accelerator Centre, (IUAC), India. We used 100 keV and 300 keV implantation energy for Ge and Xe ions, respectively, whereas the ion fluence was 1×10^{15} ions/cm^2, for both ions. The penetration depth of implanted ions was obtained by SRIM. The Ge ions showed a penetration depth of 32 nm with a straggle of 8 nm for implantation energy of 100 keV [Fig. 2 (a)], whereas a penetration ~67 nm with a straggle of 11 nm was observed for the Xe-ions with an implantation energy of 300 keV [Fig. 2 (b)]. The Raman spectra I in Fig. 1(c) and (d) illustrate the amorphization induced in the MCD film implanted with the ion fluence of 1×10^{15} ions/cm^2. The surface amorphization induced by implantation is converted into a graphitic phase because of the post-annealing process [spectra II in Fig. 1(c) and (d)]. Such a phenomenon agrees with earlier observations [39,40]. A shift of the Raman peaks from spectra I to II is also observed. The ion-implantation and annealing induced amorphization and the size effect of newly formed nano-sized graphite are responsible for shifting the Raman peaks.

After the ion-implantation, the samples were He-ion irradiated in a High Voltage Engineering Europa B.V. (HVE) particle accelerator. The energy of the He^+ ion beam was 100 keV with a fluence of 1×10^{14} ions/cm^2. Subsequently, annealing was done at 900 °C for 2 h. For implantation energy of 100 keV, the penetration depth and the straggling of He ions in MCD films were ~312.3 nm and 35.4 nm, respectively (Fig. A1). The irradiated He ions are lighter in weight compared to implanted ions. Therefore, the irradiated ions create the vacancies in the vicinity of implanted ions as well up to their penetration depth of ~312.3 nm, which is much higher than the implanted ions depth of 32 nm and 67 nm for Ge and Xe ions, respectively. As a result, the vacancies are created throughout the thickness of the diamond films. The annealing process leads to the migration of vacancies in the vicinity of substituted impurities and results in the formation of GeV and XeV color centers.

3. Results and discussions

To check the formation of the XeV and GeV centers, we performed optical characterization of the diamond samples in a home-built experimental setup where standard confocal microscopy was combined with optical spectroscopy. Our setup allows to capture photoluminescence (PL) mapping images on the XY plane of the diamond substrate as a function of depth and to perform optical spectroscopy on desired spots of the diamond substrate. Fig. 3(a) shows the schematic diagram of the optical setup. The optical beam from a diode pumped 532 nm laser is used for optical excitation. A high numerical aperture (NA = 1.3) microscope objective (MO) focuses the laser beam onto the diamond sample and also collects the PL signal which is separated from the reflected laser by a dichroic mirror (DM) and a 550 nm long pass filter, and reaches the detection part of the set-up where a Silicon Avalanche Photodiode measures the signal. For creating mapping images of the sample, the MO is mounted on a nano-positioning piezo stage which has a traveling range of 100 μm × 100 μm in XY plane and 20 μm along the Z axis. In order to measure spectra, we use a flip mirror after the DM to couple the signal to the input slit of a Andor Kymera 328i spectrograph combined with an Electron Multiplying charge-coupled device (EMCCD) camera, which has the sensitivity to detect optical signals at single photon level.

3.1. Spectroscopy characterization of the XeV centers

Fig. 3(b) exhibits a schematic representation of the possible energy states of the XeV system which were determined through earlier investigations [42,43]. It consists of a ground state G and two excited states E_1 and E_2. The non-resonant 532 nm excitation triggers the transition from the state G to A, a virtual absorption state. Subsequently, nonradiative transitions take place from the states A to the upper and lower excited states E_2 and E_1. The zero phonon lines ~794 nm and

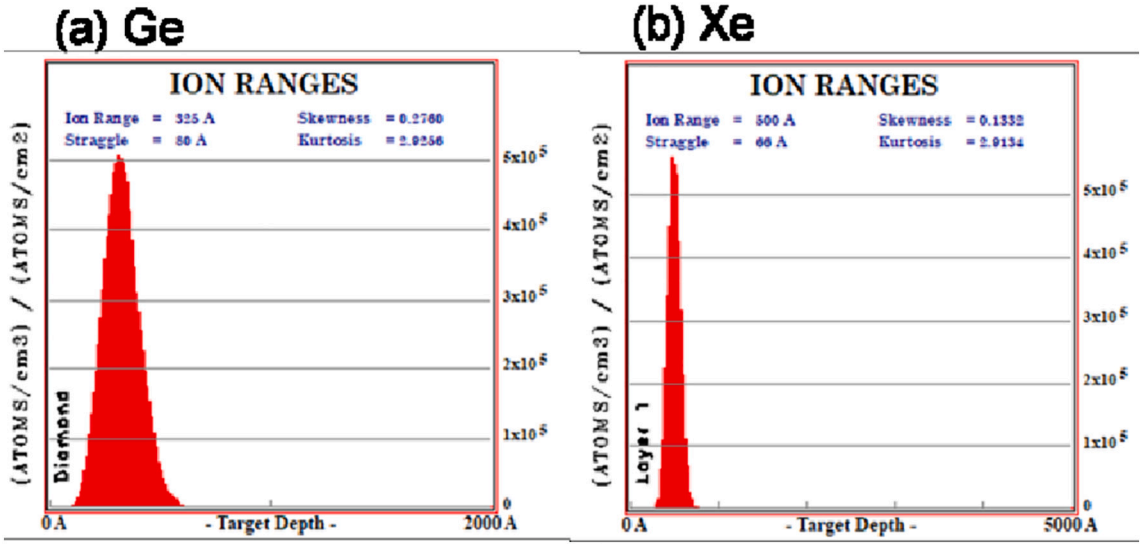

Fig. 2. SRIM results of (a) Ge ion implantation and (b) SRIM results of Xe ion implantation on MCD films.

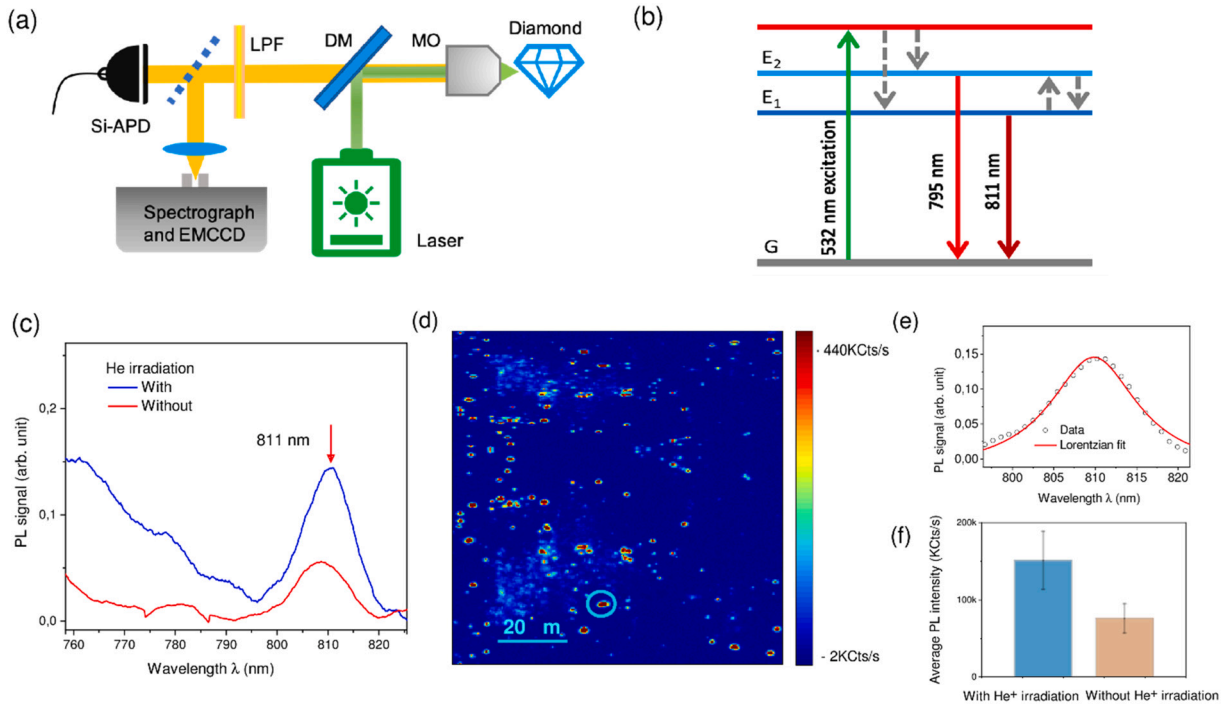

Fig. 3. (a) The schematic representation of the home-built confocal microscope which is integrated with a spectrometer. The components of the set-up are mentioned in the main text. (b) Schematic diagram of the energy levels of the XeV center. 'G' represent the ground state, E_1 and E_2 are the excited states. The arrows depict the transitions between the energy levels as described in the text. (c) Photoluminescence spectra of the implanted XeV centers which were (blue curve) and were not (red curve) subjected to He irradiation. (d) Intensity mapping image of the XeV centers in diamond. (e) Lorentzian fit to the ZPL at 811 nm for the blue curve. (f) Average intensity of the ZPL for the samples with and without He^+ irradiation. (For interpretation of the references to color in this figure legend, the reader is referred to the web version of this article.)

~811 nm are associated with the transition E_2 to G and E_1 to G, respectively. In order to examine the distribution of created XeV centers in the diamond microcrystals through ion-implantation, we measured the PL signal and generated PL mapping images. The excitation power of the laser was 0.75 mW, which was measured right before the MO. The PL mapping images revealed bright spots distributed over certain locations of the diamond substrate. To ensure the formation of XeV centers, we measured wavelength spectra of these bright spots. Fig. 3(c) (the red curve) exhibits the 811 nm ZPL in a spectrum measured for a certain bright spot. Keeping all the experimental parameters like laser power, measurement time, number of accumulation etc. fixed for the spectroscopy measurements, we captured the spectra at different spots. Although signal intensity varied in the range ~±25%, we were able to capture the ~811 nm ZPL consistently at these spots. Thus the spectroscopy data ensures successful formation of the XeV center in ion-implanted samples. However, we could not observe the ZPL ~794 nm between E_1 and G states. The 794 nm line being considerably weaker, its observation is hindered by the scattering and reflection of the signal through grain boundaries and rough surfaces of the microdiamond crystals and the existence of a strong background possibly originated from the amorphous carbon and graphite. Moreover, there is a high probability that the signal gets absorbed by sp^2 hybridized carbon atoms [44]. Although the 811 nm signal encounters the above mentioned losses, the signal being comparatively stronger [45], we were able to capture it. Next, we annealed the implanted samples at 900 °C and performed PL measurements. However, we did not observe any noticeable enhancement in the PL signal compared to the PL from the as-implanted samples.

Subsequently, after irradiating the as-implanted sample with He^+ ions and annealing at 900 °C, we performed the optical measurements again keeping the experimental parameters the same. We captured PL data for a large number of positions throughout both the samples which was and was not irradiated by He^+ ions. We observed a significant enhancement in the average PL intensity for the He^+ irradiated sample in the mapping image and in the spectroscopy data accumulated through these measurements. Fig. 3(d) exhibits a mapping image from an area of 100 μm × 100 μm. A grain-like texture appears in the map most likely due to the random inclinations and orientation of MCD facets. The optical spectrum was measured for the spot encircled in Fig. 3(d), and is shown by the blue curve in Fig. 3(d). The spectrum evidently shows the ZPL peak ~811 nm with enhanced intensity compared to the non-irradiated sample. Fig. 3(e) shows the fit of the XeV ZPL data to Lorentzian line-shape function and we observe a full width half maximum (FWHM) of 12.9 nm which is consistent with earlier reports [25,26]. MCD films grown on non-diamond substrates lead to the growth of polycrystalline diamond films with intrinsic strain, which results in the inhomogeneous broadening of ZPLs of color centers [46]. This can be a possible reason behind the broadening of XeV ZPL in Fig. 3(e). Fig. 3(f) shows average intensity of the ZPLs measured at different positions of the samples with and without He^+ irradiation. The error bars represent the standard deviations.

3.2. Spectroscopy characterization of the GeV centers

Incorporation of GeV centers in the diamond microcrystals was also investigated by combining confocal microscopy and optical spectroscopy using the optical set-up described above. Similar to SiV center [16], the energy spectrum of the GeV center also consists of a ground state ^2E_g and an excited state ^2Eu, with both levels having two-fold degeneracy. One can assign level 1, 2 to the ground and 3, 4 to the excited states, respectively as shown in Fig. 4(a). Although at low temperature it is possible to spectrally resolve the 4 to 2, 4 to 1, 3 to 2 and 3 to 1 transitions, at room temperature (RT) one can only observe a single ZPL ~602 nm. First, we performed measurements on the ion implanted sample. Although the mapping images showed bright spots distributed over the diamond substrate, the spots were not considerably bright

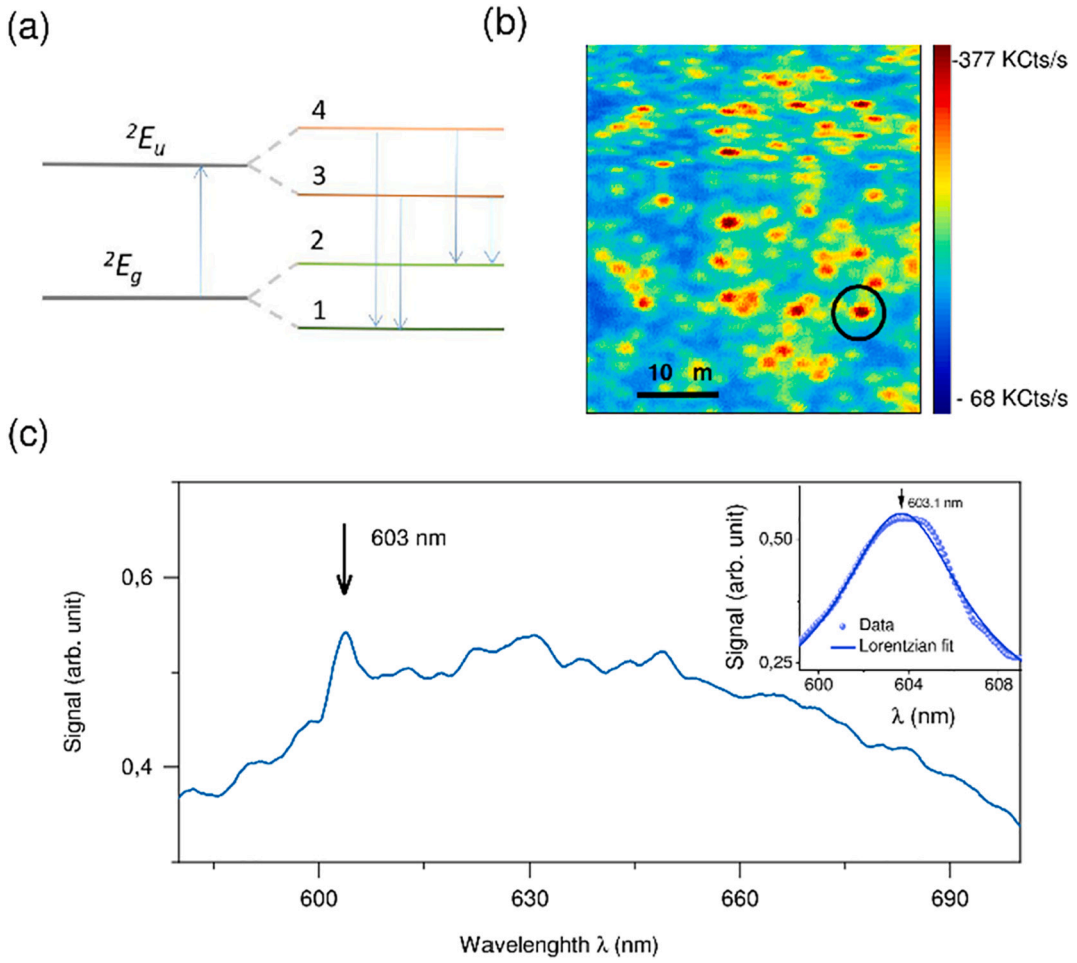

Fig. 4. (a) Schematic diagram of the energy levels of the GeV center [41]. (b) Intensity mapping image of the GeV centers measured using the confocal microscope. (c) Photoluminescence spectrum of the GeV centers marked by a circle in (b). The inset shows the background corrected ZPL data (circles) and its fit (solid curve) to Lorentzian peak function in an enlarged scale.

compared to the background. The spectra measured at these spots showed either very weak or no peak close to 602 nm, which hardly confirms the creation of GeV centers. Next, to observe any change in the optical data, we measured the He^+ irradiated sample under the same experimental conditions. The PL mapping images depicted bright spots with high contrast (SNR > 5) being distributed inhomogeneously with varying concentration throughout the sample. Fig. 4(b) shows such a mapping image. Similar to the MCD sample with XeVs, the grain-like structure in the map possibly appears due to the random distribution of the MCD surfaces in the sample. To ensure the formation of the GeV centers, we performed optical spectroscopy measurements at different bright spots. The optical spectra from different positions consistently exhibit a distinct peak around 603 nm which can clearly be attributed to the RT ZPL of the GeV center. We measured all the spectra at same excitation laser power of 2 mW. The RT PL spectrum of the encircled spot shown in Fig. 4(b), is exhibited in Fig. 4(c). Earlier observations reported that at RT the GeV ZPL appears at 602.5 nm [18], ~602 nm [19], 602.7 nm [47] etc. However in our case we see the ZPL ~603 nm. ZPL being highly sensitive to local crystal strains [48], the appearance of the peak position differs in different samples. The inset shows an enlarged view of the ZPL peak and its fit to Lorentzian line-shape, which has a FWHM of 4.5 nm which is consistent with earlier findings [19,47]. A significant enhancement in the PL intensity and consistent appearance of 603 nm peak at different positions throughout the sample suggest that He^+ irradiation and subsequent annealing have successfully created GeV centers in the MCD sample.

4. Conclusions

To conclude, we have demonstrated an engineered process of He^+ irradiation for creating XeV and GeV centers in microcrystalline diamond and enhancing their concentration. He^+ irradiation and subsequent annealing at 900 °C were performed on the Ge and Xe ion implanted diamond samples. We performed optical characterization of both without and with He^+ irradiated samples through confocal microscopy and spectroscopy. We observed clear signature of increased PL signal of XeV and GeV centers for the irradiated and annealed samples, which evidently signifies a result of He^+ irradiation.

These results open the possibility for large scale creation of GeV and XeV centers in microcrystalline diamond films which can have potential application in photonics technology. Further optimization of the preparation and process parameters will allow us to maximize the production of GeV and XeV centers with reduced cost. Moreover, since the ZPL linewidths of the XeV and GeV centers are noticeably broad, a low temperature spectroscopy study will allow us to explore their applicability in quantum technology platforms.

CRediT authorship contribution statement

TC is responsible for conceptualizing, performing the spectroscopy study, organizing and writing the manuscript. KJS is responsible for conceptualizing, performing the CVD growth and for reviewing the manuscript. KS, CHC and HN are responsible for CVD growth and for

reviewing the manuscript. RN and KA are responsible for ion implantation and for reviewing the manuscript. KH is responsible for conceptualizing and supervising the project and for revising the manuscript.

Declaration of competing interest

The authors declare that they have no known competing financial interests or personal relationships that could have appeared to influence the work reported in this paper.

Acknowledgments

This work was financially supported by the Methusalem NANO network and the Research Foundation Flanders (FWO) via SBO-project S004018N and the Special Research Fund (BOF) Postdoctoral Fellowship of KJS. We thank Milos Nesladek for his insightful suggestions. We also thank IUAC staff for their support in ion implantations.

Appendix A

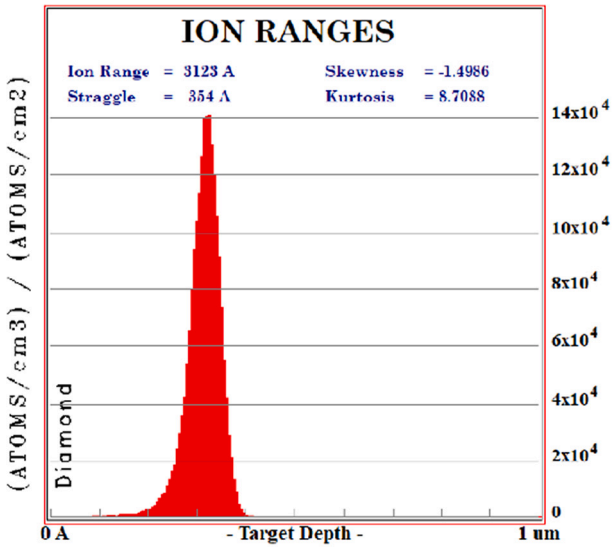

Fig. A.1. SRIM results of He^{+} ions into the MCD films.

References

[1] P. Rudolph, Handbook of Crystal Growth: Bulk Crystal Growth, Elsevier, 2014.
[2] R. Mildren, J. Rabeau, Optical engineering of diamond, John Wiley & Sons, 2013.
[3] M.W. Doherty, N.B. Manson, P. Delaney, F. Jelezko, J. Wrachtrup, L.C. L. Hollenberg, The nitrogen-vacancy colour centre in diamond, Phys. Rep. 528 (2013) 1–45, https://doi.org/10.1016/j.physrep.2013.02.001. http://www.sciencedirect.com/science/article/pii/S0370157313000562.
[4] F. Jelezko, J. Wrachtrup, Single defect centres in diamond: a review 13 (2006) 3207.
[5] H. Bernien, L. Childress, L. Robledo, M. Markham, D. Twitchen, R. Hanson, Two-photon quantum interference from separate nitrogen vacancy centers in diamond, Phys. Rev. Lett. 108 (2012), 043604.
[6] P. Neumann, N. Mizuochi, F. Rempp, P. Hemmer, H. Watanabe, S. Yamasaki, V. Jacques, T. Gaebel, F. Jelezko, J. Wrachtrup, Multipartite entanglement among single spins in diamond, Science 320 (2008) 1326.
[7] L. Rondin, J.-P. Tetienne, T. Hingant, J.-F. Roch, P. Maletinsky, V. Jacques, Magnetometry with nitrogen-vacancy defects in diamond, Rep. Prog. Phys. 77 (2014), 056503.
[8] T. Wolf, P. Neumann, K. Nakamura, H. Sumiya, T. Ohshima, J. Isoya, J. Wrachtrup, Subpicotesla diamond magnetometry, Phys. Rev. X 5 (2015), 041001.
[9] R. Schirhagl, K. Chang, M. Loretz, C.L. Degen, Nitrogen-vacancy centers in diamond: nanoscale sensors for physics and biology, Annu. Rev. Phys. Chem. 65 (2014) 83–105.
[10] S. Haziza, N. Mohan, Y. Loe-Mie, A. Lepagnol-Beste, S. Massou, M. Adam, X.L. Le, J. Viard, C. Plancon, R. Daudin, P. Koebel, E. Dorard, C. Rose, F. Hsieh, C. Wu, B. Potier, Y. Herault, C. Sala, A. Corvin, B. Allinquant, H. Chang, F. Treussart, M. Simonneau, Fluorescent nanodiamond tracking reveals intraneuronal transport abnormalities induced by brain-disease-related genetic risk factors, Nat. Nanotechnol. 12 (2017) 322.
[11] J. Wang, F. Feng, J. Zhang, J. Chen, Z. Zheng, L. Guo, W. Zhang, X. Song, G. Guo, L. Fan, C. Zou, L. Lou, W. Zhu, G. Wan, High-sensitivity temperature sensing using an implanted single nitrogen-vacancy center array in diamond, Phys. Rev. B 91 (2015), 155404.
[12] P. Neumann, I. Jakobi, F. Dolde, C. Burk, R. Reuter, G. Waldherr, J. Honert, T. Wolf, A. Brunner, J.H. Shim, D. Suter, H. Sumiya, J. Isoya, J. Wrachtrup, High-precision nanoscale temperature sensing using single defects in diamond, Nano Lett. 13 (2013) 2738–2742.
[13] E.R. Schmidgall, S. Chakravarthi, M. Gould, I.R. Christen, K. Hestroffer, F. Hatami, K.-M.C. Fu, Frequency control of single quantum emitters in integrated photonic circuits, Nano Lett. 18 (2018) 1175–1179.
[14] V. Acosta, C. Santori, A. Faraon, Z. Huang, K.-M. Fu, A. Stacey, D. Simpson, K. Ganesan, S. Tomljenovic-Hanic, A. Greentree, S. Prawer, R.G. Beausoleil, Dynamic stabilization of the optical resonances of single nitrogen-vacancy centers in diamond, Phys. Rev. Lett. 108 (2012), 206401.
[15] E. Neu, D. Steinmetz, J. Riedrich-Möller, S. Gsell, M. Fischer, M. Schreck, C. Becher, Single photon emission from silicon-vacancy colour centres in chemical vapour deposition nano-diamonds on iridium, New J. Phys. 13 (2011), 025012.
[16] C. Hepp, T. Müller, V. Waselowski, J.N. Becker, B. Pingault, H. Sternschulte, D. Steinmüller-Nethl, A. Gali, J.R. Maze, M. Atatüre, C. Becher, Electronic structure of the silicon vacancy color center in diamond, Phys. Rev. Lett. 112 (2014), 036405.
[17] J.N. Becker, J. Görlitz, C. Arend, M. Markham, C. Becher, Ultrafast all-optical coherent control of single silicon vacancy colour centres in diamond, Nat. Commun. 7 (2016) 13512.
[18] E.A. Ekimov, S. Lyapin, K.N. Boldyrev, M.V. Kondrin, R. Khmelnitskiy, V.A. Gavva, T.V. Kotereva, M.N. Popova, Germanium-vacancy color center in isotopically enriched diamonds synthesized at high pressures, JETP Lett. 102 (2015) 701–706.
[19] T. Iwasaki, F. Ishibashi, Y. Miyamoto, Y. Doi, S. Kobayashi, T. Miyazaki, K. Tahara, K.D. Jahnke, L.J. Rogers, B. Naydenov, F. Jelezko, S. Yamasaki, S. Nagamachi, T. Inubushi, N. Mizuochi, M. Hatano, Germanium-vacancy single color centers in diamond, Sci. Rep. 5 (2015) 12882.
[20] Y. Zhou, Z. Mu, G. Adamo, S. Bauerdick, A. Rudzinski, I. Aharonovich, W.-B. Gao, Direct writing of single germanium vacancy center arrays in diamond, New J. Phys. 20 (2018), 125004.
[21] E. Neu, C. Hepp, M. Hauschild, S. Gsell, M. Fischer, H. Sternschulte, D. Steinmüller-Nethl, M. Schreck, C. Becher, Low-temperature investigations of single silicon vacancy colour centres in diamond, New J. Phys. 15 (2013), 043005.
[22] K. Bray, B. Regan, A. Trycz, R. Previdi, G. Seniutinas, K. Ganesan, M. Kianinia, S. Kim, I. Aharonovich, Single crystal diamond membranes and photonic resonators containing germanium vacancy color centers, ACS Photon. 5 (2018) 4817–4822.

[23] H. Siampour, S. Kumar, V.A. Davydov, L.F. Kulikova, V.N. Agafonov, S. I. Bozhevolnyi, On-chip excitation of single germanium vacancies in nanodiamonds embedded in plasmonic waveguides, Light Sci. Appl. 7 (2018) 61.
[24] G. Keiser, Optical fiber communications, in: Wiley Encyclopedia of Telecommunications, 2003.
[25] R. Sandstrom, L. Ke, A. Martin, Z. Wang, M. Kianinia, B. Green, W.-B. Gao, I. Aharonovich, Optical properties of implanted xe color centers in diamond, Opt. Commun. 411 (2018) 182–186.
[26] A. Zaitsev, A. Bergman, A. Gorokhovsky, M. Huang, Diamond light emitting diode activated with Xe optical centers, Phys. Status Solidi A 203 (2006) 638–642.
[27] A. Bergman, A. Zaitsev, M. Huang, A. Gorokhovsky, Photoluminescence and Raman studies of Xe ion-implanted diamonds: dependence on implantation dose, J. Lumin. 129 (2009) 1524–1526.
[28] J. Meijer, B. Burchard, M. Domhan, C. Wittmann, T. Gaebel, I. Popa, F. Jelezko, J. Wrachtrup, Generation of single color centers by focused nitrogen implantation, Appl. Phys. Lett. 87 (2005), 261909.
[29] S. Pezzagna, B. Naydenov, F. Jelezko, J. Wrachtrup, J. Meijer, Creation efficiency of nitrogen-vacancy centres in diamond, New J. Phys. 12 (2010), 065017.
[30] T. Chakraborty, F. Lehmann, J. Zhang, S. Borgsdorf, N. Wöhrl, R. Remfort, V. Buck, U. Köhler, D. Suter, Cvd growth of ultrapure diamond, generation of nv centers by ion implantation, and their spectroscopic characterization for quantum technological applications, Phys. Rev. Mater. 3 (2019), 065205.
[31] C.-C. Fu, H.-Y. Lee, K. Chen, T.-S. Lim, H.-Y. Wu, P.-K. Lin, P.-K. Wei, P.-H. Tsao, H.-C. Chang, W. Fann, Characterization and application of single fluorescent nanodiamonds as cellular biomarkers, Proc. Natl. Acad. Sci. U. S. A. 104 (2007) 727–732.
[32] Y.-R. Chang, H.-Y. Lee, K. Chen, C.-C. Chang, D.-S. Tsai, C.-C. Fu, T.-S. Lim, Y.-K. Tzeng, C.-Y. Fang, C.-C. Han, H. Chang, W. Fann, Mass production and dynamic imaging of fluorescent nanodiamonds, Nat. Nanotechnol. 3 (2008) 284–288.
[33] S.C. Lawson, D. Fisher, D.C. Hunt, M.E. Newton, On the existence of positively charged single-substitutional nitrogen in diamond, J. Phys. Condens. Matter. 10 (1998) 6171.
[34] T.-L. Wee, Y.-K. Tzeng, C.-C. Han, H.-C. Chang, W. Fann, J.-H. Hsu, K.-M. Chen, Y.-C. Yu, Two-photon excited fluorescence of nitrogen-vacancy centers in proton-irradiated type ib diamond, J. Phys. Chem. A 111 (2007) 9379–9386.
[35] J.F. Ziegler, J.P. Biersack, The stopping and range of ions in matter, in: Treatise on Heavy-ion Science, Springer, 1985, pp. 93–129.
[36] R. Kumar, P. Pandit, P. Pal, S. Dhakate, R. Pant, R. Kumar, D.K. Avasthi, D.K. Singh, Engineering bright fluorescent nitrogen-vacancy (nv) nano-diamonds: role of low-energy ion-irradiation parameters, AIP Adv. 8 (2018), 085023.
[37] T.D. Merson, S. Castelletto, I. Aharonovich, A. Turbic, T.J. Kilpatrick, A. M. Turnley, Nanodiamonds with silicon vacancy defects for nontoxic photostable fluorescent labeling of neural precursor cells, Opt. Lett. 38 (2013) 4170–4173.
[38] S. Drijkoningen, P. Pobedinskas, S. Korneychuk, A. Momot, Y. Balasubramaniam, M.K. Van Bael, S. Turner, J. Verbeeck, M. Nesládek, K. Haenen, On the origin of diamond plates deposited at low temperature, Cryst. Growth Des. 17 (2017) 4306–4314, https://doi.org/10.1021/acs.cgd.7b00623.
[39] R. Kalish, Doping of diamond, Carbon 37 (1999) 781–785.
[40] S. Prawer, R. Kalish, Ion-beam-induced transformation of diamond, Phys. Rev. B 51 (1995) 15711.
[41] P. Siyushev, M.H. Metsch, A. Ijaz, J.M. Binder, M.K. Bhaskar, D.D. Sukachev, A. Sipahigil, R.E. Evans, C.T. Nguyen, M.D. Lukin, P.R. Hemmer, Y.N. Palyanov, I. N. Kupriyanov, Y.M. Borzdov, L.J. Rogers, F. Jelezko, Optical and microwave control of germanium-vacancy center spins in diamond, Phys. Rev. B 96 (2017), 081201.
[42] V. Martinovich, A. Turukhin, A. Zaitsev, A. Gorokhovsky, Photoluminescence spectra of xenon implanted natural diamonds, J. Lumin. 102 (2003) 785–790.
[43] A. Bergman, A. Zaitsev, A. Gorokhovsky, Polarization of luminescence and site symmetry of the Xe center in diamond, J. Lumin. 125 (2007) 92–96.
[44] A.M. Zaitsev, Optical Properties of Diamond: A Data Handbook, Springer Science & Business Media, 2013.
[45] Y. Deshko, A. Gorokhovsky, Spectroscopy and micro-luminescence mapping of Xe-implanted defects in diamond, Low Temp. Phys. 36 (2010) 465–471.
[46] N.B. Manson, M. Hedges, M.S. Barson, R. Ahlefeldt, M.W. Doherty, H. Abe, T. Ohshima, M.J. Sellars, Nv̄n+ pair centre in 1b diamond, New J. Phys. 20 (2018), 113037.
[47] V. Ralchenko, V. Sedov, A. Khomich, V. Krivobok, S. Nikolaev, S. Savin, I. Vlasov, V. Konov, Observation of the ge-vacancy color center in microcrystalline diamond films, Bull. Lebedev Phys. Inst. 42 (2015) 165–168.
[48] A. Batalov, V. Jacques, F. Kaiser, P. Siyushev, P. Neumann, L. Rogers, R. McMurtrie, N. Manson, F. Jelezko, J. Wrachtrup, Low temperature studies of the excited-state structure of negatively charged nitrogen-vacancy color centers in diamond, Phys. Rev. Lett. 102 (2009), 195506.